The Seventh International Colloquium on Bluff Body Aerodynamics and Applications (BBAA7)
Shanghai, China; September 2-6, 2012

# Effects of the swirl ratio on the turbulent flow fields of tornado-like vortices by using LES turbulent model

Zhenqing Liu [a], Takeshi Ishihara[b]

[a]*Department of Civil Engineering , School of Engineering, The University of Tokyo, 7-3-1, Hongo, Bunkyo-ku, Tokyo, Japan*
[b]*Department of Civil Engineering , School of Engineering, The University of Tokyo, 7-3-1, Hongo, Bunkyo-ku, Tokyo, Japan*

ABSTRACT: Tornado-like vortices have been investigated by using LES turbulence model. The flow fields are visualized by virtual water vapor injected from the ground of the numerical model and the evolution from a single-celled vortex into a multi-vortex configuration is successfully reproduced. The flow fields as well as the force balance of four typical tornado configurations, weak vortex, vortex breakdown, vortex touch-down and multi-vortex are investigated. The definitions for the swirl ratio are summarized and the local corner swirl ratio is found to be robust and proposed to universalize the researches.

KEYWORDS: Tornado-like vortex, Swirl ratio, Flow fields, LES, CFD simulation.

## 1 INTRODUCTION

Tornadoes are one of the severe natural phenomenons and considered as the most violent storm on earth, which makes it important to take proper consideration of tornado-induced wind loads and tornado-borne missiles for wind resistant design of structures. Therefore, detailed information of the three-dimensional flow fields is necessary. Many researchers are motivated to observe the wind dynamics and collect the data in real tornadoes by using velocity and pressure instrumentation. However, due to the extreme danger faced by the observers, data collection for tornado's internal flow fields is still not much of a success. Reproducing tornadoes experimentally or numerically is therefore an alternative.

Laboratory simulations provide a safe, reproducible and controllable approach for the tornado-related researches. Mitsuta and Monji (1984) modified the simulator to provide the circulation by four small fans installed in the circulation chamber. Transition of a vortex from a one-cell to two-cell structure occurred throughout the whole convergence layer in their simulator. Haan et al. (2008) developed a large laboratory simulator with guide-vanes at the top to make the translation of the tornadoes reproducible. Most recently, Tari, P.H. et al. (2010) quantified both the mean and turbulent flow fields for a range of swirl ratios spanning from F0 to F2 scale by using the Particle Image Velocimetry (PIV) method. However, in view of the limitation of observation methods and the extremely complicated flow fields near the ground, it is difficult to make detailed three-dimensional measurements in the boundary layer which has been universally believed to be the most important region in the tornado-like vortices.

Recently, with the advancement in the computer technology, many numerical studies have been conducted. Nolan and Farrell (1999) explored the dynamics of axisymmetric tornado-like vortices. The internal swirl ratio as well as the vortex Reynolds number was defined. D.C

Lewellen et al. (2000) explored some tornado structures being expected to occur in nature. They defined the local corner swirl ratio and proposed the existence of a critical swirl ratio, at which the largest swirl velocity occurs very close to the ground. Ishihara et al. (2011) used LES turbulent model to simulate the flow fields of two types of tornado-like vortices and validated the model by comparing with laboratory simulators. The formation of one-cell and two-cell type vortices were investigated by examining axisymetric time averaged Navier-Stokes equations. However, among all the simulators the definition for the swirl ratio is not uniform and varies from one to another.

In this study, a numerical model representing the Ward-type tornado simulator is built and four typical types of tornado vortices are examined. The details of this model and the case settings are introduced in section 2 including its dimension, grid distribution and boundary conditions. In section 3 the three-dimensional flow fields as well as the force balance is provided. Section 4 proposes a universal definition of swirl ratio to unify the researches.

## 2 NUMERICAL MODEL

### 2.1 *Governing equations*

The governing equations employed in LES model are obtained by filtering the time-dependent Navier-Stokes equations as follows:

$$\frac{\partial \rho \tilde{u}_i}{\partial x_i} = 0 \tag{1}$$

$$\frac{\partial}{\partial t}(\rho \tilde{u}_i) + \frac{\partial}{\partial x_j}(\rho \tilde{u}_i \tilde{u}_j) = \frac{\partial}{\partial x_j}\left(\mu \frac{\partial \tilde{u}_i}{\partial x_j}\right) - \frac{\partial \tilde{P}}{\partial x_i} - \frac{\partial \tau_{ij}}{\partial x_j} \tag{2}$$

where $\tilde{u}_i$ and $\tilde{p}$ are filtered mean velocity and filtered pressure respectively. $\rho$ is density, $\tau_{ij}$ is subgrid- scale stress and is modeled as follows:

$$\tau_{ij} = -2\mu_t \tilde{S}_{ij} + \frac{1}{3}\tau_{kk}\delta_{ij}, \quad \tilde{S}_{ij} \equiv \frac{1}{2}\left(\frac{\partial \tilde{u}_i}{\partial x_j} + \frac{\partial \tilde{u}_j}{\partial x_i}\right) \tag{3}$$

where $\mu_t$ is subgrid-scale turbulent viscosity, and $\tilde{S}_{ij}$ is the rate-of-strain tensor for the resolved scale.

Smagorinsky-Lilly model is used for the subgrid-scale turbulent viscosity,

$$\mu_t = \rho L_s^2 \left|\tilde{S}\right| = \rho L_s \sqrt{2\tilde{S}_{ij}\tilde{S}_{ij}}, \quad L_s = \min\left(\kappa\delta, C_s V^{1/3}\right) \tag{4}$$

where $L_s$ is the mixing length for subgrid-scales, $\kappa$ is the von Karman constant, 0.42, $C_s$ is Smagorinsky constant, $\delta$ is the distance to the closest wall and $V$ is the volume of a computational cell. In this study, $C_s$ is determined as 0.032 based on Oka and Ishihara (2009).

When a wall-adjacent cell is in the laminar sublayer, the wall shear stress is obtained from the laminar stress-strain relationship as follows:

$$\frac{\bar{u}}{u_\tau} = \frac{\rho u_\tau y}{\mu} \tag{5}$$

If the mesh cannot resolve the laminar sublayer, it is assumed that the centroid of the wall-adjacent cells fall within the logarithmic region of the boundary layer, and the law-of-the-wall is employed:

$$\frac{\bar{u}}{u\tau_{\tau}} = \frac{1}{k}\ln E\left(\frac{\rho u_{\tau} y}{\mu}\right) \tag{6}$$

where $\bar{u}$ is the filtered velocity tangential to wall, $u_{\tau}$ is the friction velocity and the constant $E$ is 9.793.

## 2.2 *Configurations and solution scheme*

In this study, a Ward-type simulator (Ward et al. 1972) is chosen and numerically simulated. The configurations of the numerical model are shown in Figure 1(a). Two significant geometry parameters are the height of the inlet layer, $h$, and the radius of the updraft hole, $r_o$, which are 200mm and 150mm respectively. The velocity profiles at the inlet are specified as below:

$$\begin{cases} U_{rs} = U_1\left(\dfrac{z}{z_1}\right)^{\frac{1}{n}} \\ V_{rs} = -U_{rs}\tan(\theta) \end{cases} \tag{7}$$

where, $U_{rs}$ and $V_{rs}$ are radial velocity and the tangential velocity at $r=r_s$, $n$ equals to 7, the reference velocity $U_1$ and the reference height $z_1$ are set to 0.24m/s and 0.01m respectively through matching the velocity profile in the previous study by Ishihara et al. (2011), and $\theta$ is the degree of the inflow angle.

Considering the axisymmetry of tornado-like vortex, an axisymmetric topology method is adopted, see Figure 1(b). With an intent to investigate the turbulent features quantitatively in the vicinity of the center and the region near the ground, very fine mesh is considered in the convergence region. The total mesh number is about $7.8\times10^6$. Table 1 summarizes the parameters for the mesh and the system of the PC cluster used in this study.

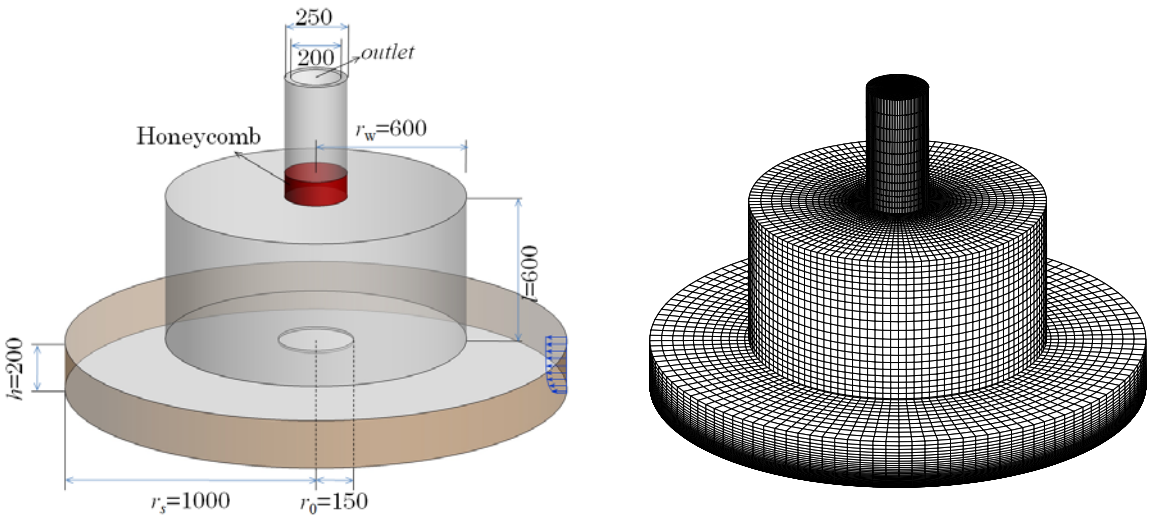


Figure 1. Geometry(a) and mesh(b) of the model.

Table 1. Parameters for the mesh and the system of PC cluster

| | |
|---|---|
| Mesh size in the radial direction | 1.0～25.0mm |
| Mesh size in the vertical direction | 0.1～5.0mm |
| Mesh number | 784200 |
| CPU | Athlon 64 Processor3200, 2.01GHz |
| Number of nodes | 8 |
| CPU time for the case of $S$=2.44 | 150h |

Finite volume method is used for the present simulations. SIMPLE (semi-implicit pressure linked equations) algorithm is employed for solving the discritized equations (Ferziger and Peric, 2002). The pressure at inlet of the convergence region is set to zero, and velocity at the outlet (0, 0, $W_0$) is given as (0, 0, 9.55m/s) to generate upward flow in the tornado. Three velocity components and the pressure are set as zero for the initial conditions.

### 2.3 *Swirl ratio definitions and Case settings*

In both the laboratory and the numerical simulators, a correlation has been found between the vortex structure and the swirl ratio. Various definitions for the swirl ratio have been proposed in the previous studies.

The swirl ratio has historically been defined as the ratio of angular momentum to radial momentum in the vortex, and expressed in the following forms:

$$S_{out}=\frac{\Gamma_\infty r_0}{2Qh},\ S_{out}=\frac{\Gamma_\infty}{2Qa}\ \text{and}\ S_{out}=\frac{\tan\theta}{2a} \tag{8}$$

where, $\Gamma_\infty$is the circulation at the outer edge of the convergence region, $\Gamma_\infty=2\pi r_s h V_\infty$, and $a$ is the aspect ratio, $a=h/r_0$. In case the circulation is imposed by using guide vanes instead of rotating screen, the ratio of the circulation rate to the volume flow rate can easily be replaced by tan$\theta$, where $\theta$ is the angle of the guide vanes.

In ISU tornado simulator by F. L. Haan Jr.(2008) the swirl ratio is specifically modified as:

$$S=\frac{r_c\Gamma_c}{2Qh}=\frac{r_c(2\pi r_c V_c)}{2Q}=\frac{\pi r_c^2 V_c}{Q} \tag{9}$$

in which, the circulation, $\Gamma_c$, is estimated using the multiplication of the maximum tangential velocity, $V_c$, and $r_c$, $\Gamma_c=2\pi r_c h V_c$, $r_c$ is radius of maximum tangential velocity, $V_c$, in the quasi-cylindrical region.

D.C. Lewellen(2000) proposed a local corner flow swirl ratio, $S_c$. The specific form of the local corner flow swirl ratio is:

$$S_c=\frac{r_c^*\Gamma_\infty^{*2}}{\Upsilon} \tag{10-a}$$

in which, $r_c^*$ is the characteristic length scale, calculated as $r_c^*\equiv\Gamma_\infty^*/V_c$, $2\pi\Gamma_\infty^*$ is the circulation per unit height in the outer region expressed as $2\pi\Gamma_\infty^*=2\pi V_\infty r_\infty$, $\Upsilon$ is the total depleted circulation flux flowing through the corner flow region, expressed as:

$$\Upsilon\approx 2\pi\int_0^{r_2} W(r,z_2)\,\Gamma_d(r,z_2)\,r\,dr \tag{10-b}$$

where, $\Gamma_d$ is the depleted angular momentum and defined as $\Gamma_d=\Gamma_\infty-Vr$, $r_2$ is the radius safely outside of the upper-core region, $z_2$ is the height just above the corner flow.

Table 2. Case settings and accompany tornado vortex parameters.

| Case | $\theta$ (°) | $S_{out}$ | $S$ | $S_c$ | $Re$ | $Q$(m$^3$/s) | $V_c$ (m/s) | $r_c$ (m) |
|---|---|---|---|---|---|---|---|---|
| Case1 | 46.8 | 0.4 | 0.02 | 0.71 | $1.6\times10^5$ | 0.30 | 10.72 | 0.014 |
| Case2 | 58.0 | 0.6 | 0.06 | 1.59 | $1.6\times10^5$ | 0.30 | 9.84 | 0.024 |
| Case3 | 64.9 | 0.8 | 0.12 | 2.36 | $1.6\times10^5$ | 0.30 | 9.11 | 0.035 |
| Case4 | 69.4 | 1 | 0.23 | 2.93 | $1.6\times10^5$ | 0.30 | 9.62 | 0.047 |
| Case5 | 76.0 | 1.5 | 0.34 | 4.16 | $1.6\times10^5$ | 0.30 | 10.99 | 0.054 |
| Case6 | 79.4 | 2 | 0.69 | 5.39 | $1.6\times10^5$ | 0.30 | 12.35 | 0.073 |
| Case7 | 82.1 | 2.7 | 1.06 | 6.74 | $1.6\times10^5$ | 0.30 | 14.26 | 0.084 |
| Case8 | 83.5 | 3.3 | 1.58 | 7.96 | $1.6\times10^5$ | 0.30 | 15.98 | 0.105 |
| Case9 | 84.4 | 3.8 | 2.44 | 8.89 | $1.6\times10^5$ | 0.30 | 18.62 | 0.112 |
| Previous | 60.0 | 0.65 | 0.08 | 3.05 | $1.6\times10^5$ | 0.30 | 8.33 | 0.030 |

Notes:

- Case1, Case2, Case4 and Case9 are four typical types of tornado configuration and are chosen for detailed flow field analysis.
- Previous case is the simulation carried out by Ishihara (2011).

In this study, the swirl ratio is increased through increasing the inflow angle. Nine cases are calculated systematically. The case settings as well as tornado vortex parameters for each case are illustrated in Table 2, in which $Re$ is the Reynolds number defined as $Re=W_0D/\upsilon$, $D=2r_0$. It can be found the swirl ratio $S_{out}$ tends to have a larger value compared with $S$. On the other hand, the local corner swirl ratio $S_c$ shows the maximum value for the same corner flow pattern.

## 3 FLOW FIELDS CHARACTERISTICS

It is necessary to make the air flow visible and evaluate the vortex in a qualitative manner. For this purpose virtual water vapor is selected as the visualizing substance injected from the bottom of the model. The particles are not released until the flow fields are in the quasi-steady stage to eliminate the effect of the transit field solution.

As the value of the swirl ratio is increased, the vortex goes through various stages, as depicted in Figure 2. When $S$=0.02, we find the central core to have a smooth, laminar appearance. The core extends upward from the surface to the high elevation spreading radially slightly with height, shown in Figure 2(a). For $S$=0.06, a "vortex breakdown" occurs where the flow transitions from a tight, laminar vortex to a broader, turbulent state, see Figure 2(b). At $S$=0.23, the radius of the vortex core increases and the altitude of the breakdown decreases, as shown in Figure 2(c). The vortex breakdown is just above the boundary layer. A still further increase in swirl ratio to $S$=2.44 results in the breakdown being forced further toward the surface layer, see Figure 2(d). The core of the vortex expands substantially, leaving a relatively calm inner subcore. Concurrent with the expansion of the core the inner downflow penetrates to the lower surface, and in this particular snapshot, a family of several secondary vortices rotating about the main vortex is evident.

### 3.1 *Mean flow fields*

Quantitative analysis can be achieved by examining the distributions of the mean velocity components. In the following discussion, the maximum tangential velocity in the cyclostrophic balance region, $V_c$, will be used to normalize the flow fields. The radial distance is normalized by the core radius of the tornado vortex in cyclostrophic balance region, $r_c$.

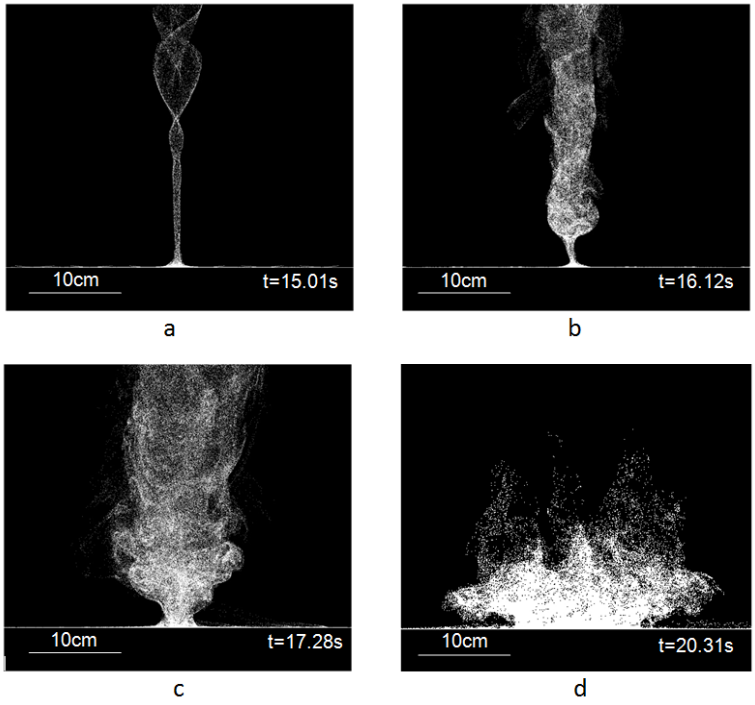


Figure 2. Flow visualization by injecting water vapor from the ground for four typical types of tornado-like vortices, (a) weak vortex, S=0.02, (b) vortex breakdown, S=0.06, (c) vortex touch-down, S=0.23, (d) multi-vortex, S=2.44.

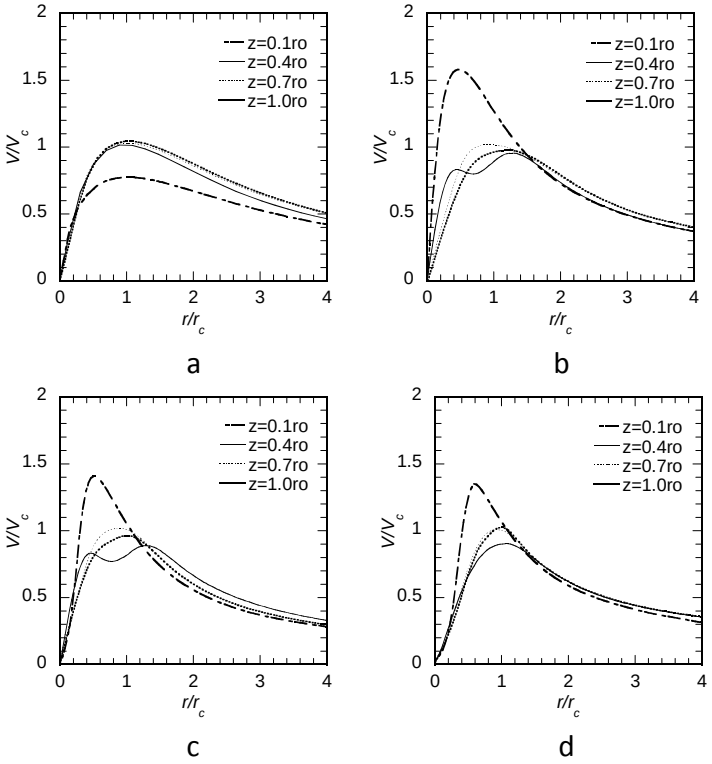


Figure 3. Radial profiles of the normalized tangential velocity for four typical types of tornado-like vortices, (a) weak vortex, S=0.02, (b) vortex breakdown, S=0.06, (c) vortex touch-down, S=0.23, (d) multi-vortex, S=2.44.

The radial profiles of the mean tangential velocity, $V$, versus nondimensional radial distance are shown in Figure 3(a). For the very low swirl ratio case, $S$=0.02, the mean tangential velocity field is apparently one dimensional except the layer very near the ground. The core radius, $R$, defined based on the location of the maximum tangential velocity at each elevation, is almost consistent. For $S$=0.06, the swirl overshoot appears at the surface layer with maximum tangential velocity being 1.6 times of $V_c$, and the core radius increases from $0.5r_c$ to $1.0r_c$ with height forming a funnel shape. Further increasing the swirl ratio to the stages of touch-down and multi-vortex, the ratio of maximum swirl velocity, $V_{max}$, to $V_c$ is nearly a constant, varying in between 1.3 to 1.5, and the radial location of $V_{max}$ changes very slightly, holding about $0.5r_c$.

### 3.2 *Force balances analysis*

The contributions from each term in Navier-Stokes equation can be calculated by force balances analysis. Ishihara, T. (2011) investigated the force balances of two typical stages by using the time-averaged axisymmetric Navier-Stokes equations. However, a systematic cross comparison for the force balances in various types of vortices is limited and deserved to be studied.

The time-averaged radial Navier-Stokes equation can be expressed as:

$$U\frac{\partial U}{\partial r}+W\frac{\partial U}{\partial z}-\frac{V^2}{r}=-\frac{1}{\rho}\frac{\partial P}{\partial r}-\left(\frac{\partial u^2}{\partial r}+\frac{\partial uw}{\partial z}-\frac{v^2}{r}+\frac{u^2}{r}\right)+D_u \tag{11}$$

The left hand side consists of the radial advection term, $A_{ru}$, the vertical advection term, $A_{zu}$, as well as the centrifugal force term, $C_r$. The right hand side of the equation is the radial pressure

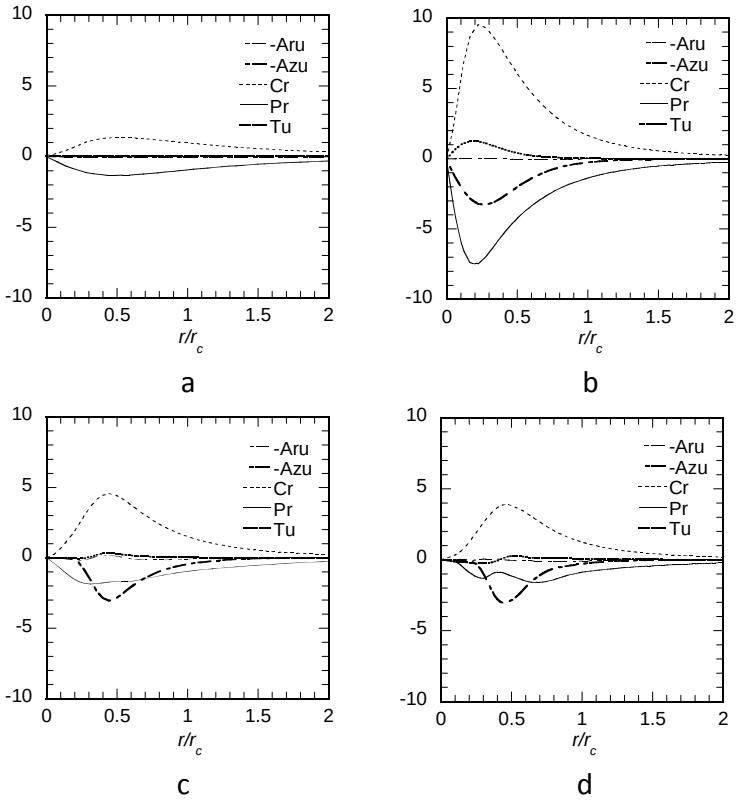


Figure 4. Radial force for four typical types of tornado-like vortices, (a) weak vortex, S=0.02, (b) vortex breakdown, S=0.06, (c) vortex touch-down, S=0.23, (d) multi-vortex, S=2.44.

gradient term, $P_r$, turbulent force term, $T_u$, and the diffusion term, $D_u$. The diffusion term, $D_u$, in the equation is small enough to be ignored compared with the other terms. $u$,$v$,$w$ are root mean squares of the radial, tangential and vertical velocities.

Due to the slight change for the height of maximum tangential velocity, the terms in the radial momentum equations are computed at $z$=0.1$r_o$ as a function of $r/r_c$ for all the four stages, as shown in Figure 4. Examination of Figure 4(a) reveals that turbulence plays little role for weak vortex stage in the radial momentum balance. The centrifugal term and pressure gradient term are the significant portion of the total balance. Increasing the swirl to $S$=0.06, the flow evolves from laminar vortex to a turbulent state, followed by a significant change of the radial balance, as shown in Figure 4(b). The principle balance is in between the centrifugal term, pressure gradient term, turbulent term and vertical advective term. The emergence of the turbulent term is the manifestation of the unsteadiness of the flow fields. Figure 4(c) displays the terms in the radial balance for the case of vortex touch-down. The centrifugal term is mainly balanced by the pressure gradient term as well as the vertical advective term. However, different with the state of vortex breakdown, in some region the vertical advection term becomes more important than the pressure gradient term. Radial force balance for multi-vortex is presented in Figure 4(d), which is almost coincident with that for vortex touch-down.

## 4 PERFORMANCE OF LOCAL CORNER SWIRL RATIO

A pictorial approach is adopted to show how the surface intensification and the shape of the vortices change with the swirl ratio $S_c$, as illustrated in Figure 5, where $U_{min}$ is the minimum averaged radial velocity, $V_{max}$ is the maximum averaged tangential velocity, $W_{max}$ is the maximum vertical velocity, $r_{vmax}$ and $h_{vmax}$ are the radius and height of the location of the maximum tangential velocity respectively. The parameters $V_{max}/V_c$, $-U_{min}/V_{max}$, $W_{max}/V_{max}$ and the ratio of $r_{vmax}$ to $h_{vmax}$ are examined. The results of this study will be compared with the previous laboratory-scale numerical study by Ishihara et al. (2011) and the full scale numerical study by Lewellen et al. (2000). It is worth to be mentioned that the methods to obtain the angular momentum are different from one to another. In the previous study by Ishihara et al. (2011), the azimuthal momentum of the inflow is imposed by guide vanes, while in the present 8 cases the circulation is obtained directly from the velocity profile at the inlet boundary. For the full scale numerical model by Lewellen et al. (2000), the boundary condition is obtained from an inner nest of a thunderstorm simulation.

The ratio of the maximum averaged swirl velocity, $V_{max}$, to the maximum averaged swirl velocity in the upper cyclostrophic region, $V_c$, as a function of the local corner swirl ratio is demonstrated in Figure 5(a). Examining the set of present cases, the ratio increases sharply from the very low swirl ratio until $S_c$ equals to around 1.6 where the pattern of vortex breakdown occurs and the distinct peak ratio reaches to about 1.7. For increasing the swirl ratio, the ratio of $V_{max}$ to $V_c$ decreases moderately and at last becomes almost a constant varying the values in between 1.3 and 1.5.

Figure 5(b) shows the ratio $-U_{min}/V_{max}$ as a function of the local corner swirl ratio. This ratio increases suddenly from the state of weak vortex, however, it is obvious that, except the very low swirl cases, $-U_{min}/V_{max}$ is insensitive to the swirl ratio and all the data are scattered about a central value 0.65. This near consistency is the indication of the dependency between the low-level radial overshoot and the swirl overshoot.

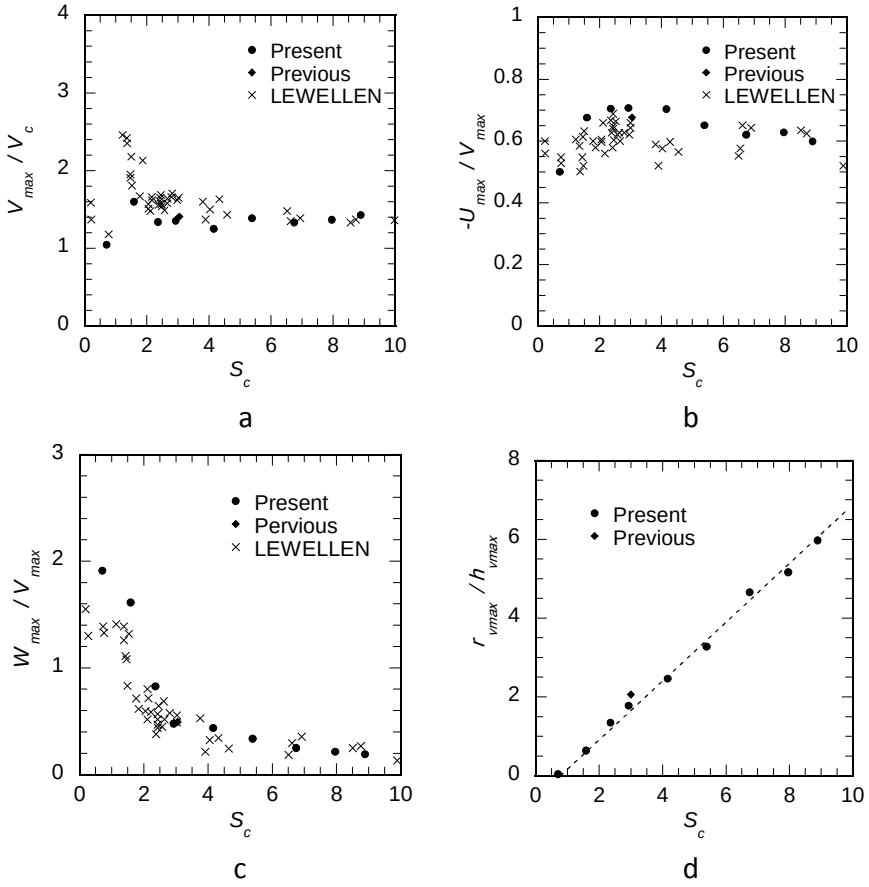


Figure 5. Summery surface intensification and the geometry of tornado vortices as a function of local corner swirl ratio, (a) the ratio of $V_{max}/V_c$, (b) the ratio of $-U_{min}/V_{max}$, (c) the ratio of $W_{max}/V_{max}$ and (d) the aspect ratio of $r_{vmax}/h_{vmax}$.

The ratio $W_{max}/V_{max}$ shows the maximum value, about 1.9, at the stages with very low swirl ratios, and decreases with increasing the swirl ratio, as demonstrated in Figure 5(c). The maximum vertical velocity is larger than the maximum tangential velocity until the vortex reaches to the touch-down state, after which the near consistency for the ratio $W_{max}/V_{max}$ is observed with a central value of about 0.4.

A vortex aspect ratio defined as the ratio of $r_{vmax}$ to $h_{max}$ is applied to evaluate the structure of the flow in the vortex corner. As observed in Figure 5(d), the vortex aspect ratio increases linearly with $S_c$ having a slope of about 0.7.

The values of $V_{max}/V_c$, $-U_{min}/V_{max}$ and $W_{max}/V_{max}$ as a function of local corner swirl ratio obtained in Lewellen et al. (2000) and Ishihara et al. (2011) are also shown for comparison. Even though the present, previous and Lewellen's cases use different numerical models to generate the vortices, it is obvious that the results from different models exhibit the universally same tendencies. Therefore it can be argued that it is reasonable to universalize the researches by using the local corner swirl ratio.

## 5 CONCLUSIONS

The flow fields as well as the force balances of tornado-like vortices have been investigated by using the LES turbulent model in this study. Following summarizes the conclusions.

1. The visualized flow fields by the injected water fog from the ground successfully show the evolution from a single-celled vortex into a two-cell vortex configuration containing multiple subsidiary vortices.

2. The maximum normalized tangential velocity occurs at the stage of vortex breakdown, after which the maximum tangential velocity almost holds as a constant and the normalized radial location of $V_{max}$ changes very slightly. Turbulence plays little role for weak vortex stage in the radial momentum balance. From the stage of vortex breakdown the force balance changes dramatically and the effects of turbulence emerge.

3. The values of $V_{max}/V_c$, $-U_{min}/V_{max}$ and $W_{max}/V_{max}$ obtained from different simulators are plotted as a function of local corner swirl ratio and show good comparison. The vortex aspect ratio $r_{vmax}/h_{rvmax}$ shows linear relationship with the local corner swirl ratio having a slope of about 0.7. Based on the consistency provided by the local corner swirl ratio, it is proposed to universalize the researches.

## REFERENCES

1 Ferziger, J. and Peric, M., Computational method for fluid dynamics, 3rd Edition, , 2002, Springer.
2 Haan, F.L., Sarkar, P.P., Gallus, W.A., Design, construction and performance of a large tornado simulator for wind engineering applications, Engineering Structures, 2008, Vol.30, pp.1146-1159.
3 Ishihara, T., Oh, S., and Tokuyama, Y., Numerical study on flow fields of tornado-like vortices using the LES turbulence model, Journal of Wind Engineering and Industrial Aerodynamics, 2011, Vol.99, pp.239-248.
4 Lewellen, D.C., Lewellen, W.S., and Sykes, R.I., Large-eddy simulation of a tornado's interaction with the surface, Journal of the Atmospheric Sciences, 1997, Vol.54, pp.581-605.
5 Lewellen, D.C., Lewellen, W.S., and Xia. J., The influence of a local swirl ratio on tornado intensification near the surface, Journal of the Atmospheric Sciences, 2000, Vol.57, pp.527-544.
6 Mitsuta,Y. and Monji, N., Development of a laboratory simulator for small scale atmospheric vortices, Natural Disaster Science, 1984, Vol.6, pp.43-54.
7 Nolan, D.S. and Farrell, B.F., The structure and dynamics of tornado-like vortices, Journal of the Atmospheric Sciences, 1999, Vol.56, pp.2908-2936.
8 Oka,S. and Ishihara,T., Numerical study of aerodynamic characteristics of a square prism in a uniform flow. Journal of Wind Engineering and Industrial Aerodynamics, 2009, Vol.97, pp.548–559.
9 Tari, P.H., Gurka, R., Hangan, H.. Experimental investigation of tornado-like vortex dynamics with swirl ratio: The mean and turbulent flow fields, Journal of Wind Engineering and Industrial Aerodynamics, 2010, Vol.98, pp.936-944.
10 Ward, N.B., The Exploration of Certain Features of Tornado Dynamics Using a Laboratory Model, Journal of the Atmospheric Sciences, 1972, Vol.29, pp.1194-1204.